projected separation between the X-ray peak and optical centroids, we further limited the subsample to systems that have such a separation of less than 12 kpc. In total, there are 49 systems (32 for the B55 and 41 for the HIFLUGCS) that meet these criteria ($\eta_{\rm min} < 5$ and separation < 12 kpc), 31 of which have detected bubbles (22 for the B55, 26 for the HIFLUGCS). Table 2 lists the systems that meet these criteria and also lack detected bubbles.

Finally, based on the central cooling time (at 1 kpc) and the separation (see Fig. 2), we also consider a somewhat larger subsample: those systems with central cooling times below $\sim 10^9$ yr and separations smaller than 12 kpc. This subsample includes the previous main heating subsample, plus seven extra systems (see Table 2). There are a total of 56 systems (39 for the B55 and 47 for the HIFLUGCS) in this extended subsample. Therefore, there are 16 systems in the B55 and 16 systems in the HIFLUGCS (19 systems in total) that are excluded from the samples of systems that need heating.

5.2 Simulations

For the systems without bubbles from our extended subsample (which have cooling times at 1 kpc smaller than $\sim 10^9$ yr), we performed simulations in order to find the locations and the sizes of bubbles that can be present in the cluster and remain undetected. These systems are listed in Table 2.

No attempt was made to simulate the effects of bright rims around the bubbles, since that would complicate the model greatly. When present, these can enhance bubble contrast, making them more evident. As a result, if undetected bubbles had bright rims, we may be overestimating their possible energy content. Regardless of this, the modelling used here provides good limits on the energy that may be contained in undetected bubbles.

We simulated a three-dimensional cluster using a spherically symmetric β profile model for the emissivity (derived from the existing archive observations, see Table 2). The parameters of the β model were fixed to those derived from the azimuthally averaged surface brightness profiles. When a double-β model was preferred over a single-β model, the double-β model was used in the simulation. A cube of $500 \times 500 \times 500$ elements was populated with the corresponding emissivities.

For simplicity, spherical bubbles were simulated in this cube by setting the emissivities inside the bubbles to zero. However, it is important to note that observationally it is unclear whether the X-ray cavities are devoid of X-ray emitting gas or instead are filled with hot, underdense gas. Then, by integrating the emissivity along lines of sight through the cube, we obtained the two-dimensional surface brightness map. This map was used as input for the MARX simulator[3] in order to obtain a simulated *Chandra* image. For MARX we used a spectrum extracted from the data, with the integration time and position set as in the data. As in the case of the systems from Section 2.2, we used the CIAO tool *merge_all* to add all the available observations for each system. This total integration time is used in the simulations (see Table 2 for details).

We assume that the bubbles expand adiabatically into a β-model atmosphere. Therefore, the radius of the bubble at the distance r from the centre of the cluster is given by

$$R_{\rm b}(r) = R_{\rm b}(0)\left[1 + \left(\frac{r}{r_{\rm c}}\right)^2\right]^{3\beta/10}, \quad (4)$$

where $R_{\rm b}(0)$ is the bubble size at the cluster centre, $r_{\rm c}$ is the core radius and β is the parameter of the beta model. To calculate the ages we assume that the bubbles rise buoyantly from the centre of the cluster to their current radius (giving $t_{\rm buoy}$, see Section 2.2 for details). In order to calculate the initial size, $R_{\rm b}(0)$, with which the bubbles are injected, we assumed: $4pV \sim P_{\rm cav}t \sim L_{\rm X}t$, where p is the central pressure of the cluster, $L_{\rm X}$ is the bolometric X-ray luminosity inside $r_{\rm cool}$ (see Section 3) and t is the time between the outbursts. We adopted a time between outbursts of 10^8 yr, motivated by the observations of clusters with multiple generations of bubbles, such as Perseus (Fabian et al. 2000). We ran multiple simulations for a cluster, with the locations of the bubbles and the angle in the plane of sky (ϕ) randomized, and with an angle from the line of sight (θ) of 90°. The resulting images were inspected to determine if the bubbles remain visible for the whole of the 10^8 yr outburst cycle. If a bubble becomes undetectable when its buoyancy age was less than 10^8 yr, such a bubble may be present, but undetectable, in the real cluster and the heating rate could be sufficient to balance cooling. In cases where the bubble would have remained visible for the whole cycle, the simulation was repeated using smaller values of $P_{\rm cav}$, until the bubble becomes undetectable in less than 10^8 yr. Under our assumptions, this value of $P_{\rm cav}$ determines an upper limit on the possible AGN power in such systems. These systems are A3112, A1650, A1689, RXCJ 1504.1−0248, A2244 and Ophiuchus. Therefore, these systems have upper limits less than the value required to balance cooling under our assumptions (see Table 2).

5.3 Biases in bubble samples

Samples of observed bubbles could suffer from biases due to detectability and projection effects. To assess the degree to which such biases might be present, we simulated an A4059-like cluster with two bubbles with a variety of sizes and positions. We then attempted to detect the bubbles by eye (without knowing their locations or sizes a priori). The measured properties can then be compared to the intrinsic ones to understand possible biases.

In total, 89 simulations were performed. Bubble radii were varied between 10 and 60 kpc, and the distance from the core to the bubble was varied between 20 and 80 kpc. Bubbles with radii greater than the bubble-to-core distance were not simulated. Fig. 3 (left) shows a comparison between the measured bubble radii and the true ones. Approximately 44 per cent of the simulated bubbles were undetected. Of these, the majority had an axis between the bubble and core that was oriented near to the line of sight ($\theta \lesssim 45°$) or were small bubbles at large distances from the core. Of those that were detected, the measured bubble radius is on average close to the true one. The greatest deviations from equality are generally for bubbles with smaller angles to the line of sight.

A similar situation also applies to the comparison between the measured distance to the core and the true one, shown in Fig. 3 (right). It is clear that most of the undetected bubbles lie at large distances from the core or, again, have small values of θ. For detected bubbles, the average distance is close to the true one in most cases. These results imply that when bubbles are detected, their properties are probably not grossly in error, particularly in an average sense.

Lastly, we can estimate the detection rate for bubbles as a function of bubble radius and distance to the core by summing over all angles of the bubble-to-core axis to the line of sight. This detection rate is shown in Fig. 4. As expected, the detection fraction depends strongly on the bubble size and on the distance from the core.

[3] See http://www.space.mit.edu/CXC/MARX/

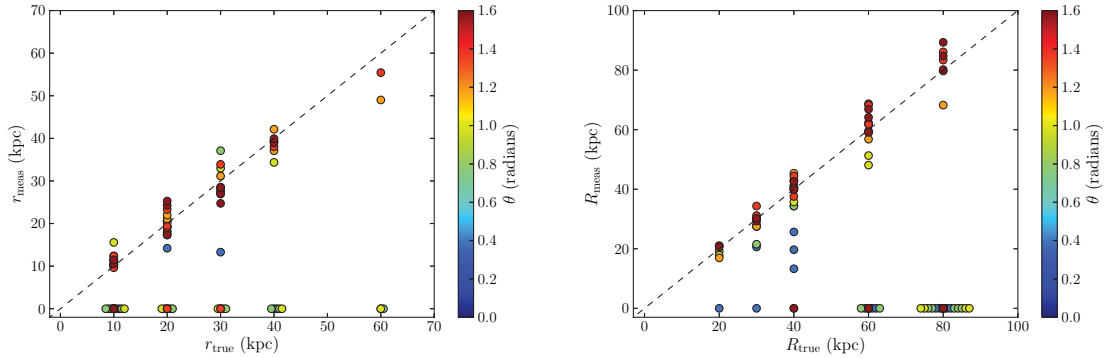

Figure 3. Left: measured bubble radius versus the true radius. The colour denotes the value of θ, the angle between the bubble-to-core axis and the line of sight. Undetected bubbles are shown at a measured radius of zero. Right: measured distance from the core to the bubble versus the true distance.

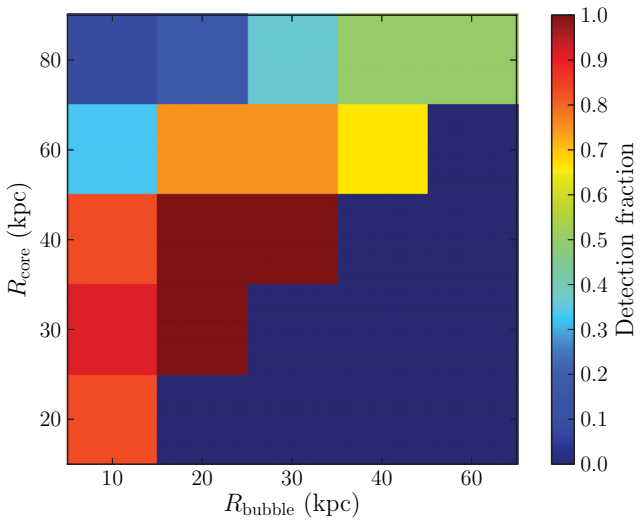

Figure 4. Detection fraction as a function of the true bubble radius and the true (unprojected) distance from the bubble centre to the cluster core. The fraction has been summed over all angles between the bubble-to-core axis and the line of sight.

However, it is currently unclear as to which fraction of real bubbles are expected to fall into this parameter space.

5.4 The duty cycle

Fig. 5 shows the bubble power (the heating rate) versus the bolometric X-ray luminosity (the cooling rate) within the cooling radius (at which $t_{cool} < 7.7 \times 10^9$ yr) for our sample of cooling flows. The fraction of systems with detected bubbles for the main subsample is ≈0.69 (22/32) for the B55 and ≈0.63 (26/41) for the HIFLUGCS. We note that this sample is based on two criteria: $\eta_{min} < 5$ and X-ray-to-optical core separation <12 kpc. If, however, the AGN are not fuelled by cooled gas, then the η_{min} criterion is not relevant to this analysis. For the larger samples based on cooling time cut-off, the fraction is ≈0.56 (22/39) for the B55 and ≈0.55 (26/47) for the HIFLUGCS. This implies a duty cycle in cooling flows of at least 55–69 per cent. This duty cycle agrees well with previous findings (Dunn et al. 2006; Nulsen et al. 2009; Dong et al. 2010) and with the radio-loud fraction of BCGs in cooling flows (Burns 1990). It also agrees with the radio-loud fraction of ∼30 per cent found for massive galaxies by Best et al. (2005), when adjusted for the fraction of such systems that are in cooling flows (∼50 per cent, see Section 5.1).

From Fig. 5 we can conclude that most of the systems that lack detected bubbles could have enough bubble power to balance cooling and remain undetected in existing images. A few systems have upper limits on the bubble power below the $4pV$ line, implying that they cannot have sufficient bubble power to balance cooling under our assumptions. However, one of our primary assumptions is that the bubbles are in the plane of the sky. As noted in Section 1, the orientation of the bubble axis relative to the line of sight has a strong effect on the detectability of the bubbles. If the angle from the bubble axis to the line of sight is $\lesssim 30^\circ$, it is difficult to detect even large bubbles. As such an orientation is expected to occur in roughly 15 per cent of all systems (assuming the jet axes are randomly oriented), it is possible that approximately two to three of the systems without detected bubbles in our sample have significant bubble power that is hidden. Unfortunate orientation might therefore account for all of the systems for which the upper limit on the bubble power is insufficient to balance cooling. Therefore, with existing data, one cannot exclude the scenario that almost all cooling-flow clusters have bubbles with enough power to balance cooling, implying a duty cycle for such activity of up to 100 per cent.

However, of the seven intermediate CFs (with a central cooling time between ∼5 and 10 × 10^8 yr), only A2063 shows extended radio emission. Thus, if the remaining intermediate systems do have bubbles, they must be 'ghost', like those of A2597 (McNamara et al. 2001). It is more probable that these systems have previously had a cooling core that was heated by a merger, such as A2142, A3571, A1651, A2244 and corona system A576 (see Section 6.4). Therefore, these systems might not need bubbles in order to balance the internal heating.

Also, it is important to mention that some of the systems without bubbles are corona-class systems (denoted by the blue symbols in Fig. 5), which often have large radio lobes (all such systems in our sample except A576, MKW 8, A2589 and A3558 have lobes) embedded in lower density gas surrounding the bright X-ray core, which reduces the contrast of any bubbles and makes them harder to detect. Such systems may well have undetected bubbles. They include A400, A3376, A2634, A3395s, Coma and 3C129.1.

However, it is not fully understood what makes these systems different from larger cooling cores or whether the radio-mode feedback cycle applies to them. Since the radio lobes are inflated beyond the cooling region and the fraction of the outburst energy coupled to the corona is small, their feedback process may be very

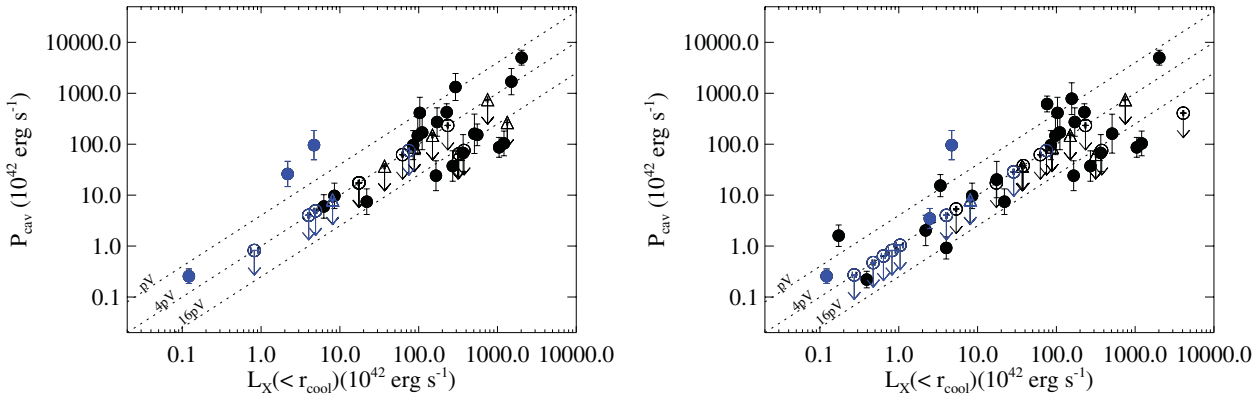

Figure 5. Bubble power versus the X-ray luminosity (inside the cooling region) for the subsamples of systems that require heating from the B55 (left-hand panel) and the HIFLUGCS (right-hand panel). The subsample of systems that require heating is listed in Table 2 (see Section 5.1 for details). Different symbols denote different subsamples: the circles for the main subsample ($\eta_{\rm min} < 5$ and separation < 12 kpc) and the triangles for the extended sample (cooling time at 1 kpc between 0.5 and 1 Gyr and separation < 12 kpc). The filled symbols denote the systems with bubbles and the blue symbols denote the corona-class systems, which are marked with an asterisk in Table 2. The diagonal lines indicate $P_{\rm cav} = L_{\rm X}$ assuming pV, $4pV$ or $16pV$ as the energy deposited. The limits on the $4pV$ line are not strictly upper limits, but simply mark the systems where the limit is at least this large.

inefficient, and heating required to balance the internal cooling might be supplied by supernovae or by heat conduction (Sun et al. 2007). Alternatively, radio heating through weak shocks may be important in these systems (for a discussion on the importance of weak shocks for AGN heating, see the review of McNamara & Nulsen 2012). When the corona class systems are excluded, we find a duty cycle of 76 per cent ($= (22 - 3)/(32 - 7)$) for the B55 main subsample and 77 per cent ($= (26 - 3)/(41 - 11)$) for the HIFLUGCS main subsample.

Lastly, we find that the fraction of systems with detected bubbles for both complete samples is very similar. The two subsamples overlap for 44 systems (see Section 2.1); however, the HIFLUGCS extends to lower mass systems. In general, our results are most relevant for clusters, since there are only 10 ellipticals and poor clusters in our sample (three for the B55 and nine for the HIFLUGCS) and eight of them have bubbles.

6 DISCUSSION

6.1 Radio luminosity cut-off

Fig. 1 (left) shows that there is a radio luminosity cut-off for massive clusters, such that systems with a central radio luminosity above 2.5×10^{30} erg s^{-1} Hz^{-1} are found only in cooling flows (see Section 4.1). This supports the idea that the radio-mode outbursts are self-regulating, with increased radio luminosity (and hence feedback power) seen in sources where cooling is likely occurring.

We also note that the luminosity of central radio sources does not appear to be lower on average when there are no detected bubbles. In such systems, the radio source lacks bright lobes and is core dominated but is generally as bright as the systems with radio lobes and bubbles. This is the case of A1689, A1644 and RXCJ 1504.1−0248, which represent ∼10 per cent of the high-luminosity objects (see Section 6.3). A1689 is an interesting case, as it is not part of the main subsample since it has a thermal stability parameter much higher than 5, and it has a radio halo (Vacca et al. 2011). This system may have been heated up by a major merger (Andersson & Madejski 2004) that did not destroy the cool core.

6.2 Duty cycle of radio-mode feedback

As discussed in Section 5.4, our simulations imply an AGN heating duty cycle of at least ∼60 per cent and up to 100 per cent. This result implies that CFs do not undergo long periods of time in which no significant cavities are present in their hot atmospheres. Therefore, it appears from our results that the atmospheres of cooling flows are undergoing almost non-stop energy injection through bubbles inflated by the central AGN. The exact nature of this heating remains unclear (for a review, see McNamara & Nulsen 2007), but our results clearly point to a connection between the presence of gas that is unstable to cooling (traced by low values of $\eta_{\rm min}$) and the bubbles. This connection supports the idea that cold gas accretion, which might be induced by mergers or cooling of the ICM, fuels the outbursts that create the bubbles instead of hot accretion (i.e. Bondi accretion).

The heating duty cycle that we have derived is distinct from the jet duty cycle, which is the fraction of time that the radio jet is active. Our results do not address the jet duty cycle, which, when traced only by the bubble population, could range from small values if the jets operate in short, intermittent bursts (which inflate the cavities and then stop) to values approaching unity if instead the jets are continuous (and the bubbles detach from them as they rise). However, we found that almost every source with cooling time below $\sim 5 \times 10^8$ yr has radio lobes. Our results should be useful as constraints on (or inputs to) simulations that include radio-mode AGN heating.

6.3 Cooling-flow systems without bubbles

Fig. 1 (left) shows that the systems with bubbles have short cooling times ($\lesssim 5 \times 10^8$ yr) and the majority of them have high radio luminosities ($\gtrsim 2.5 \times 10^{30}$ erg s^{-1} Hz^{-1}). However, as discussed in the previous section, some systems with short cooling times do not appear to have bubbles (e.g. Rafferty et al. 2008). Here, we further examine these systems to understand whether they are likely to have bubbles that are simply missed in observations. In particular, we examine their radio properties, star formation properties and merger activity.

When the radio luminosity is considered, we find that many of the objects with high radio luminosity ($\gtrsim 2.5 \times 10^{30}$ erg s^{-1} Hz^{-1}) that do not show bubbles in the existing *Chandra* images are 'coronae' (Sun et al. 2007; Sun 2009). In this category are A400, A3376, A2634, A3395s and Coma. The only coronae from this category for which we found bubbles are A3391 and A3532. However, all these coronae have large radio lobes (Owen et al. 1985; Becker, White & Helfand 1995; Bock, Large & Sadler 1999; Venturi et al. 2001; Hardcastle, Sakelliou & Worrall 2005; Bagchi et al. 2006). The interaction between these radio lobes and the ICM is expected to create bubbles, as in A3391 and A3532, but deeper X-ray images are needed to detect any bubbles embedded in the low-density gas of these systems. Another object with high radio luminosity, short cooling time and no visible bubbles in the existing *Chandra* image is EXO 0423.4−0840, which has a radio source at the centre of the cluster with very small lobes (Belsole, Birkinshaw & Worrall 2005). Again, the interaction between these lobes and the ICM might create bubbles, but we are not able to see the bubbles because the *Chandra* point spread function is too large to resolve them.

The remaining category of objects that have high radio luminosity, but lack bubbles, are massive clusters. This may be the case for A1644, A3112 and RXCJ 1504.1−0248. Except possibly A3112 (Takizawa et al. 2003), these systems lack radio lobes. Therefore, these systems may well lack substantial bubbles, with the possible exception of A3112, which has the shortest cooling time and some hints of radio lobes.

These systems may be in a cooling stage, between AGN outbursts. Binney & Tabor (1995) postulated that there may be short bursts of nuclear activity alternating with periods of quiescent cooling. While A3112 shows very little star formation (Hicks, Mushotzky & Donahue 2010), RXCJ 1504.1−0248 has a very high star formation rate (Rafferty et al. 2008; Ogrean et al. 2010) and a minihalo (Giacintucci et al. 2011a) most probably related to the cooling-flow activity, as in Perseus (Gitti, Brunetti & Setti 2002). A1644 also has high rates of star formation (Crawford et al. 1999; O'Dea et al. 2010). Furthermore, sloshing might provide enough heat to balance the inner cooling of the gas (ZuHone et al. 2010; ZuHone, Markevitch & Lee 2011b). This may be the case for A1644 which is thought to be undergoing a merger between the main cluster and a subcluster (Reiprich et al. 2004; Johnson et al. 2010).

The CFs with a radio luminosity below 2.5×10^{30} erg s^{-1} Hz^{-1} are mostly ellipticals, groups or poor clusters (e.g. NGC 1550, NGC 4636, NGC 507, NGC 5044, Fornax, MKW 4, AWM 7, A262 and A133) and most of them show bubbles in the existing *Chandra* images, except AWM 7, which is probably undergoing a merger (Peletier et al. 1990) and MKW 4. Both AWM 7 and MKW 4 do not have any lobe radio emission, but they have star formation activity (McNamara & O'Connell 1989), and thus they might be in a cooling stage, as proposed above for the more massive clusters like RXCJ 1504.1−0248.

Another category of cooling-flow objects with low radio luminosity are the corona class systems: A1060, III ZW 54, 3C 129.1, A3558, A2589 and MKW 8. For A1060 and III Zw 54 we measured bubbles (see Section 2.2) and 3C 129.1 has extended radio emission, and thus might have bubbles that are not visible in the existing shallow *Chandra* image. On the other hand, MKW 8, A2589 and A3558 do not have extended radio lobes (see Table 5).

There are also massive clusters with low radio luminosity: Ophiuchus, A1650 and A2065. The central galaxies in these clusters only show unresolved nuclear radio emission and no star formation, but A2065 and Ophiuchus might be in the midst of mergers (see Table 5). Also Ophiuchus has a radio minihalo (Govoni et al. 2009; Murgia et al. 2010a) and shows evidence of sloshing in its core (Million et al. 2010), which might be related (ZuHone et al. 2011a). As in the case of RXCJ 1504.1−0248, the minihalo in Ophiuchus might be related to the previous cooling-flow activity, and the sloshing has revived this old radio emission. Furthermore, Eckert et al. (2008) and Nevalainen et al. (2009) show evidence of possible hard X-ray emission, which might be of non-thermal origin, caused by Compton scattering of cosmic microwave background radiation by the same population of relativistic electrons responsible for the minihalo emission. As a result, Ophiuchus, A1650 and A2065 might be similar to the intermediate class systems, those with a cooling time between ∼5 and 10×10^8 yr, which presently are not expected to have bubbles since they are heated by major mergers, but may previously have had cooling-flow activity and bubbles (see Section 6.4).

Lastly, we note that small bubbles may be present in these systems but missed in current observations. Most of the B55 and the HIFLUGCS systems are at moderate redshifts (around $z = 0.05$), with a few systems above a redshift of 0.1 (A1689 and RXC J1504.1−0248). Therefore, bubbles such as those seen in M87 (e.g. Forman et al. 2005) would be too small to image. For example, if we extrapolate one of the inner cavities from M87, with a radius of 12 arcsec (Forman et al. 2005), to a higher redshift of 0.05 we will obtain a radius of 1 arcsec. As a result, this kind of bubble would be completely missed in current X-ray observations.

6.4 Cooling-flow versus non-cooling-flow systems

The CF/NCF dichotomy has been studied a great deal recently using observations (e.g. Sanderson et al. 2006, 2009; Chen et al. 2007; Cavagnolo et al. 2009; Pratt et al. 2009; Hudson et al. 2010) and simulations (e.g. Burns et al. 2008; McCarthy et al. 2008; Poole et al. 2008; Guo & Oh 2009). Using a statistically selected sample, Sanderson et al. (2009) found that the dichotomy seems to be real and not an archival bias. There are two main underlying origins for the CF/NCF dichotomy. The first assumes that the separation occurs early due to pre-heating (McCarthy et al. 2008) through mergers (Poole et al. 2008; Burns et al. 2008) or from TeV gamma-rays from blazars (Pfrommer, Chang & Broderick 2012). The second interpretation assumes that the separation occurs late, such that a CF cluster can be destroyed due to merger (Rossetti & Molendi 2010; Rossetti et al. 2011) or powerful AGN outburst (Guo & Oh 2009). However, Pfrommer et al. (2012) argue that the AGN heating is likely insufficient to turn a CF into an NCF cluster, but the impact of AGN-induced turbulence could result into an NCF atmosphere on time-scale larger than 1 Gyr (Parrish, Quataert & Sharma 2010; Ruszkowski & Oh 2010).

From Figs 1 (left-hand panel) and 2, we found that clusters are separated into two different groups based on the central cooling time, central source radio luminosity and the separation between the X-ray peak and the optical centroid. Clusters with low central cooling times ($\lesssim 5 \times 10^8$ yr) and smaller separation ($\lesssim$12 kpc) have a cooling-flow activity and many of them show bubbles in their atmospheres. Clusters with longer cooling times ($\gtrsim 10^9$ yr), low central radio luminosities ($\lesssim 2.5 \times 10^{30}$ erg s^{-1} Hz^{-1}) and larger separations (above 12 kpc) often show large haloes and relics likely due to merger shocks.

For the CFs, most have visible bubbles or have extended radio emission from the central source (e.g. A3112), or appear to be in a cooling stage (e.g. A1644 and RXCJ 1504.1−0248). The systems with a cooling time between $\sim 5 \times 10^8$ and 10^9 yr (A576, A2244,

A3571, A2142, A2065, A2063, A1651 and A4038) do not have visible bubbles. This result agrees with the findings of Rafferty et al. (2008), since they are above the threshold for the onset of star formation (and hence significant cooling is probably not occurring). For the central radio source, none of them have more than point-like central radio emission (see Table 5), except A2063 which has small radio lobes and possible cavities (Kanov, Sarazin & Hicks 2006). Due to the fact that most of them are experiencing some sort of merger activity, diffuse emission might also be present in some of them, such as A2142, A3571 and A4038 [see Table 5 for references and M. Rossetti (private communication) for the detection of a radio halo in A2142].

Among the eight clusters with intermediate cooling times, only A2063 and A1651 lack the central temperature decrease typical of cooling-flow clusters (see Table 4 and Section 3.2). Therefore, these systems share properties of both CF and NCFs, and thus may represent an intermediate class of systems which are presently heated by a major merger but previously might have had a cooling-flow activity and bubbles. However, one cannot say whether they will evolve towards non-cooling flow as Rossetti et al. (2011) have suggested, or if they might restart the cycle of cooling and heating again at some point.

Lastly, for the objects with central cooling times above $\sim 10^9$ yr, none show any extended emission for the central radio source, except A2147 which shows small lobes (see Table 5), and they do not have visible bubbles. A2147 might have been a corona system which was destroyed by the merger (Sun et al. 2007). However, this process has low probability even for corona systems (Sun et al. 2007). All these systems with a central cooling time above $\sim 10^9$ yr might be experiencing major mergers due to the continuing growth of large-scale structure. Therefore, they are classified as NCFs for which one does not expect the presence of bubbles.

We can conclude that CFs (including the intermediate systems) and NCFs are well separated, especially when we look at the central cooling time versus the separation between the X-ray peak and the optical core (see Fig. 2). Furthermore, the intermediate systems separate from the CFs, with a central cooling time below $\sim 5 \times 10^8$ yr, if we look at the central radio luminosity (see Fig. 1, left) and the presence of an extended central radio source (see Table 5). The intermediate systems have a radio luminosity below 2.5×10^{30} erg s^{-1} Hz^{-1} and they do not have extended central radio sources. However, from observations there is no conclusive way to know if a cluster like A2256 will become a CF (or if an object like A2065 will become a non-cooling-flow one).

The merging NCF systems and the CF systems are quite separate in Fig. 1. Thus, any transitions between the two types must be rare and/or fast. However, a transition from CF to NCF caused by a major merger or a very powerful AGN outburst was found to be improbable (Poole et al. 2008; Pfrommer et al. 2012). Transitions in the opposite direction could be the result of gas cooling or the injection of low entropy gas during a merger. However, the speed of the former process is determined by the cooling time of the central gas, while it remains unclear whether the latter process is possible since the turbulence at the cluster centre is sustained for several Gyr after a cluster merger (Paul et al. 2011). Further simulations are required to establish which, if any, of these transitions are physically plausible and could be consistent with the data.

7 CONCLUSIONS

The duty cycle of radio-mode feedback was determined for two overlapping, complete samples of cooling-flow clusters: the B55 and the HIFLUGCS. All members of both samples have been observed with *Chandra*. As a result, these observations allow us with certainty to put limits on the non-detection of bubbles in some systems and to detect more bubbles in others. We found bubbles in seven systems that were not previously reported (NGC 507, III Zw 54, NGC 1550, A496, A3391, A1060 and A3532).

We identified a total of 49 CFs (32 for the B55 and 41 for the HIFLUGCS) using two criteria: $\eta_{\rm min} < 5$ and X-ray to optical core separation < 12 kpc. However, we caution that $\eta_{\rm min}$ is relevant to AGN heating only if the AGN is fuelled by cooled gas (as opposed to accretion of hot gas, i.e. Bondi accretion). Our results imply that $\sim$60 per cent of all clusters are cooling flows: $\sim$57 per cent for the B55 and $\sim$64 per cent for the HIFLUGCS. These numbers agree well with the result of Hudson et al. (2010) for the HIFLUGCS of 72 per cent. If we exclude the corona systems (13 in total, 7 for the B55 and 11 for the HIFLUGCS), the percentage of CFs is $\sim$45 per cent ($\sim$45 per cent for the B55 and $\sim$47 per cent for the HIFLUGCS). Out of 49 CFs, 31 have bubbles (22 for the B55 and 26 for the HIFLUGCS). There are seven intermediate CFs (seven for the B55 and six for the HIFLUGCS) and none of them have bubbles. Therefore, the duty cycle of radio-mode feedback is at least $\sim$69 per cent for the B55 and $\sim$63 per cent for the HIFLUGCS. If we exclude the corona class systems, we found a duty cycle of $\sim$76 per cent for the B55 and $\sim$77 per cent for the HIFLUGCS.

We found that the more luminous central radio sources (those with $L_{1400} \gtrsim 2.5 \times 10^{30}$ erg s^{-1} Hz^{-1}) are only found in cooling flows (as are the X-ray bubbles). This result supports the AGN feedback scenario, in which cooling from the hot atmosphere results in AGN outbursts (traced by their luminous radio emission) that in turn heat the gas and prevent periods of intense, long-duration cooling.

However, some bubbles could be missed in existing observations. For the systems without detected bubbles, we used simulations to limit the energy that could be present in undetected bubbles, finding that the power being injected by the central AGN into most of these systems could balance cooling, although the bubbles remain undetected. Therefore, with the existing data, one cannot exclude the possibility that all cooling-flow clusters have bubbles with enough power to balance cooling, implying a duty cycle of up to $\sim$100 per cent. This result needs to be investigated further, especially using radio observations, to see if all cooling-flow clusters have radio lobes that might create bubbles.

ACKNOWLEDGMENTS

LB's work at Pennsylvania State University was supported by *Chandra* X-ray grant AR9-0018x. PEJN's work was supported in part by NASA grant NAS8-03060. LB thanks George Pavlov and Niel Brandt for their support at Pennsylvania State University and J. Nevalainen and D. Eckert for useful discussions about the Ophiuchus Cluster.

REFERENCES

Andersson K. E., Madejski G. M., 2004, ApJ, 607, 190
Arnaud K. A., 1996, in Jacoby G. H., Barnes J., eds, ASP Conf. Ser. Vol. 101, Astronomical Data Analysis Software and Systems V. Astron. Soc. Pac., San Francisco, p. 17
Ascasibar Y., Markevitch M., 2006, ApJ, 650, 102
Bacchi M., Feretti L., Giovannini G., Govoni F., 2003, A&A, 400, 465
Bagchi J., Durret F., Neto G. B. L., Paul S., 2006, Sci, 314, 791
Baldi A., Forman W., Jones C., Kraft R., Nulsen P., Churazov E., David L., Giacintucci S., 2009, ApJ, 707, 1034
Baum S. A., O'Dea C. P., 1991, MNRAS, 250, 737

Becker R. H., White R. L., Helfand D. J., 1995, ApJ, 450, 559
Belsole E., Birkinshaw M., Worrall D. M., 2005, MNRAS, 358, 120
Berrington R. C., Lugger P. M., Cohn H. N., 2002, AJ, 123, 2261
Best P. N., Kauffmann G., Heckman T. M., Brinchmann J., Charlot S., Ivezić Ž., White S. D. M., 2005, MNRAS, 362, 25
Binney J., Tabor G., 1995, MNRAS, 276, 663
Binney J., Tremaine S., 1987, Galactic Dynamics. Princeton Univ. Press, Princeton, NJ
Binney J., Bibi F. A., Omma H., 2007, MNRAS, 377, 142
Bîrzan L., Rafferty D. A., McNamara B. R., Wise M. W., Nulsen P. E. J., 2004, ApJ, 607, 800
Bîrzan L., McNamara B. R., Nulsen P. E. J., Carilli C. L., Wise M. W., 2008, ApJ, 686, 859
Blanton E. L., Sarazin C. L., McNamara B. R., Wise M. W., 2001, ApJ, 558, L15
Bock D., Large M. I., Sadler E. M., 1999, AJ, 117, 1578
Bravo-Alfaro H., Cayatte V., van Gorkom J. H., Balkowski C., 2000, AJ, 119, 580
Brentjens M. A., 2008, A&A, 489, 69
Brüggen M., Scannapieco E., Heinz S., 2009, MNRAS, 395, 2210
Buote D. A., Humphrey P. J., Stocke J. T., 2005, ApJ, 630, 750
Burgett W. S. et al., 2004, MNRAS, 352, 605
Burns J. O., 1990, AJ, 99, 14
Burns J. O., Roettiger K., Ledlow M., Klypin A., 1994, ApJ, 427, L87
Burns J. O., Hallman E. J., Gantner B., Motl P. M., Norman M. L., 2008, ApJ, 675, 1125
Carilli C. L., Perley R. A., Dreher J. W., Leahy J. P., 1991, ApJ, 383, 554
Carretti E. et al., 2012, preprint (arXiv:e-prints)
Cavagnolo K. W., Donahue M., Voit G. M., Sun M., 2008, ApJ, 683, L107
Cavagnolo K. W., Donahue M., Voit G. M., Sun M., 2009, ApJS, 182, 12
Cavaliere A., Fusco-Femiano R., 1976, A&A, 49, 137
Chatzikos M., Sarazin C. L., Kempner J. C., 2006, ApJ, 643, 751
Chen Y., Reiprich T. H., Böhringer H., Ikebe Y., Zhang Y., 2007, A&A, 466, 805
Churazov E., Forman W., Jones C., Böhringer H., 2003, ApJ, 590, 225
Clarke T. E., Ensslin T. A., 2006a, AJ, 131, 2900
Clarke T. E., Ensslin T., 2006b, Astron. Nachr., 327, 553
Clarke T. E., Blanton E. L., Sarazin C. L., 2004, ApJ, 616, 178
Clarke T. E., Sarazin C. L., Blanton E. L., Neumann D. M., Kassim N. E., 2005, ApJ, 625, 748
Clarke T. E., Blanton E. L., Sarazin C. L., Anderson L. D., Gopal-Krishna, Douglass E. M., Kassim N. E., 2009, ApJ, 697, 1481
Condon J. J., Cotton W. D., Greisen E. W., Yin Q. F., Perley R. A., Taylor G. B., Broderick J. J., 1998, AJ, 115, 1693
Cortese L., Gavazzi G., Boselli A., Iglesias-Paramo J., Carrasco L., 2004, A&A, 425, 429
Cotton W. D. et al., 2009, ApJ, 701, 1872
Crawford C. S., Allen S. W., Ebeling H., Edge A. C., Fabian A. C., 1999, MNRAS, 306, 857
Croton D. J. et al., 2006, MNRAS, 365, 11
David L. P. et al., 2011, ApJ, 728, 162
Davis D. S., Mushotzky R. F., 1993, AJ, 105, 409
de Plaa J. et al., 2006, A&A, 452, 397
de Ruiter H. R., Parma P., Fanti C., Fanti R., 1986, A&AS, 65, 111
Deiss B. M., Reich W., Lesch H., Wielebinski R., 1997, A&A, 321, 55
Diehl S., Li H., Fryer C. L., Rafferty D., 2008, ApJ, 687, 173
Donahue M., Voit G. M., O'Dea C. P., Baum S. A., Sparks W. B., 2005, ApJ, 630, L13
Dong R., Rasmussen J., Mulchaey J. S., 2010, ApJ, 712, 883
Donnelly R. H., Markevitch M., Forman W., Jones C., Churazov E., Gilfanov M., 1999, ApJ, 513, 690
Donnelly R. H., Forman W., Jones C., Quintana H., Ramirez A., Churazov E., Gilfanov M., 2001, ApJ, 562, 254
Dunn R. J. H., Fabian A. C., 2004, MNRAS, 355, 862
Dunn R. J. H., Fabian A. C., Taylor G. B., 2005, MNRAS, 364, 1343
Dunn R. J. H., Fabian A. C., Sanders J. S., 2006, MNRAS, 366, 758
Dunn R. J. H., Allen S. W., Taylor G. B., Shurkin K. F., Gentile G., Fabian A. C., Reynolds C. S., 2010, MNRAS, 404, 180
Dupke R. A., Mirabal N., Bregman J. N., Evrard A. E., 2007a, ApJ, 668, 781
Dupke R., White R. E., III, Bregman J. N., 2007b, ApJ, 671, 181
Durret F., Lima Neto G. B., Forman W., 2005, A&A, 432, 809
Eckert D., Produit N., Paltani S., Neronov A., Courvoisier T. J.-L., 2008, A&A, 479, 27
Eckert D., Molendi S., Paltani S., 2011, A&A, 526, A79
Edge A. C., Stewart G. C., Fabian A. C., Arnaud K. A., 1990, MNRAS, 245, 559
Edge A. C., Stewart G. C., Fabian A. C., 1992, MNRAS, 258, 177
Enßlin T. A., Heinz S., 2002, A&A, 384, L27
Fabian A. C., 1994, ARA&A, 32, 277
Fabian A. C. et al., 2000, MNRAS, 318, L65
Fabian A. C., Sanders J. S., Allen S. W., Crawford C. S., Iwasawa K., Johnstone R. M., Schmidt R. W., Taylor G. B., 2003, MNRAS, 344, L43
Fabian A. C., Sanders J. S., Taylor G. B., Allen S. W., 2005, MNRAS, 360, L20
Fabian A. C., Sanders J. S., Taylor G. B., Allen S. W., Crawford C. S., Johnstone R. M., Iwasawa K., 2006, MNRAS, 366, 417
Feretti L., Dallacasa D., Govoni F., Giovannini G., Taylor G. B., Klein U., 1999, A&A, 344, 472
Feretti L., Fusco-Femiano R., Giovannini G., Govoni F., 2001, A&A, 373, 106
Feretti L., Orrù E., Brunetti G., Giovannini G., Kassim N., Setti G., 2004, A&A, 423, 111
Finoguenov A., Henriksen M. J., Miniati F., Briel U. G., Jones C., 2006, ApJ, 643, 790
Finoguenov A., Sarazin C. L., Nakazawa K., Wik D. R., Clarke T. E., 2010, ApJ, 715, 1143
Forman W. et al., 2005, ApJ, 635, 894
Forman W. et al., 2007, ApJ, 665, 1057
Fujita Y., Matsumoto T., Wada K., 2004, ApJ, 612, L9
Gastaldello F., Buote D. A., Temi P., Brighenti F., Mathews W. G., Ettori S., 2009, ApJ, 693, 43
Ge J. P., Owen F. N., 1993, AJ, 105, 778
Gentile G., Rodríguez C., Taylor G. B., Giovannini G., Allen S. W., Lane W. M., Kassim N. E., 2007, ApJ, 659, 225
Ghizzardi S., Rossetti M., Molendi S., 2010, A&A, 516, A32
Giacintucci S. et al., 2005, A&A, 440, 867
Giacintucci S., Markevitch M., Brunetti G., Cassano R., Venturi T., 2011a, A&A, 525, L10
Giacintucci S. et al., 2011b, ApJ, 732, 95
Giovannini G., Feretti L., 2000, New Astron., 5, 335
Giovannini G., Feretti L., Venturi T., Kim K., Kronberg P. P., 1993, ApJ, 406, 399
Giovannini G., Cotton W. D., Feretti L., Lara L., Venturi T., 1998, ApJ, 493, 632
Gitti M., Brunetti G., Setti G., 2002, A&A, 386, 456
Govoni F., Enßlin T. A., Feretti L., Giovannini G., 2001, A&A, 369, 441
Govoni F., Murgia M., Feretti L., Giovannini G., Dallacasa D., Taylor G. B., 2005, A&A, 430, L5
Govoni F., Murgia M., Markevitch M., Feretti L., Giovannini G., Taylor G. B., Carretti E., 2009, A&A, 499, 371
Gregorini L., de Ruiter H. R., Parma P., Sadler E. M., Vettolani G., Ekers R. D., 1994, A&AS, 106, 1
Guo F., Oh S. P., 2009, MNRAS, 400, 1992
Hanisch R. J., 1984, A&A, 131, 276
Hardcastle M. J., Sakelliou I., 2004, MNRAS, 349, 560
Hardcastle M. J., Sakelliou I., Worrall D. M., 2005, MNRAS, 359, 1007
Harris D. E., Bahcall N. A., Strom R. G., 1977, A&A, 60, 27
Hayakawa A., Furusho T., Yamasaki N. Y., Ishida M., Ohashi T., 2004, PASJ, 56, 743
Henriksen M. J., 1993, ApJ, 414, L5
Henriksen M. J., Tittley E. R., 2002, ApJ, 577, 701
Henry J. P., Finoguenov A., Briel U. G., 2004, ApJ, 615, 181
Hicks A. K., Mushotzky R., Donahue M., 2010, ApJ, 719, 1844
Hudson D. S., Reiprich T. H., Clarke T. E., Sarazin C. L., 2006, A&A, 453, 433

Hudson D. S., Mittal R., Reiprich T. H., Nulsen P. E. J., Andernach H., Sarazin C. L., 2010, A&A, 513, A37
Johnson R. E., Markevitch M., Wegner G. A., Jones C., Forman W. R., 2010, ApJ, 710, 1776
Johnston-Hollitt M., 2003, PhD thesis, Univ. Adelaide
Johnston-Hollitt M., Sato M., Gill J. A., Fleenor M. C., Brick A., 2008, MNRAS, 390, 289
Johnstone R. M., Fabian A. C., Morris R. G., Taylor G. B., 2005, MNRAS, 356, 237
Kale R., Dwarakanth K. S., 2009, ApJ, 699, 1883
Kale R., Dwarakanath K. S., 2010, ApJ, 718, 939
Kanov K. N., Sarazin C. L., Hicks A. K., 2006, ApJ, 653, 184
Kassim N. E., Clarke T. E., Enßlin T. A., Cohen A. S., Neumann D. M., 2001, ApJ, 559, 785
Kawaharada M., Makishima K., Kitaguchi T., Okuyama S., Nakazawa K., Matsushita K., Fukazawa Y., 2009, ApJ, 691, 971
Kempner J. C., David L. P., 2004, ApJ, 607, 220
Kempner J. C., Sarazin C. L., Ricker P. M., 2002, ApJ, 579, 236
Kim D.-W., Fabbiano G., 1995, ApJ, 441, 182
Kim K.-T., Kronberg P. P., Giovannini G., Venturi T., 1989, Nat, 341, 720
Krawczynski H., Harris D. E., Grossman R., Lane W., Kassim N., Willis A. G., 2003, MNRAS, 345, 1255
Krempec-Krygier J., Krygier B., 1999, Acta Astron., 49, 403
Krempeć-Krygier J., Krygier B., Krywult J., 2002, Baltic Astron., 11, 269
Lal D. V., Rao A. P., 2004, A&A, 420, 491
Lane W. M., Kassim N. E., Ensslin T. A., Harris D. E., Perley R. A., 2002, AJ, 123, 2985
Lane W. M., Clarke T. E., Taylor G. B., Perley R. A., Kassim N. E., 2004, AJ, 127, 48
Lara L., Feretti L., Giovannini G., Baum S., Cotton W. D., O'Dea C. P., Venturi T., 1999, ApJ, 513, 197
Leonard A., King L. J., Goldberg D. M., 2011, MNRAS, 413, 789
Lindblad P. O., Jorsater S., Sandqvist A., 1985, A&A, 144, 496
Macario G., Markevitch M., Giacintucci S., Brunetti G., Venturi T., Murray S. S., 2011, ApJ, 728, 82
Markevitch M., Vikhlinin A., 2001, ApJ, 563, 95
Markevitch M., Vikhlinin A., 2007, Phys. Rep., 443, 1
Markevitch M. et al., 2000, ApJ, 541, 542
Markevitch M., Vikhlinin A., Mazzotta P., 2001, ApJ, 562, L153
Mathews W. G., Brighenti F., 2008, ApJ, 685, 128
Mauch T., Murphy T., Buttery H. J., Curran J., Hunstead R. W., Piestrzynski B., Robertson J. G., Sadler E. M., 2003, MNRAS, 342, 1117
McCarthy I. G., Babul A., Bower R. G., Balogh M. L., 2008, MNRAS, 386, 1309
McNamara B. R., Nulsen P. E. J., 2007, ARA&A, 45, 117
McNamara B. R., Nulsen P. E. J., 2012, New J. Phys., 14, 055023
McNamara B. R., O'Connell R. W., 1989, AJ, 98, 2018
McNamara B. R. et al., 2000, ApJ, 534, L135
McNamara B. R. et al., 2001, ApJ, 562, L149
McNamara B. R., Wise M. W., Murray S. S., 2004, ApJ, 601, 173
McNamara B. R., Nulsen P. E. J., Wise M. W., Rafferty D. A., Carilli C., Sarazin C. L., Blanton E. L., 2005, Nat, 433, 45
Miller N. A., 2005, AJ, 130, 2541
Miller N. A., Owen F. N., 2003, AJ, 125, 2427
Miller N. A., Owen F. N., Hill J. M., 2003, AJ, 125, 2393
Million E. T., Allen S. W., Werner N., Taylor G. B., 2010, MNRAS, 405, 1624
Mittal R., Hudson D. S., Reiprich T. H., Clarke T., 2009, A&A, 501, 835
Morganti R., Oosterloo T., Tadhunter C. N., Aiudi R., Jones P., Villar-Martin M., 1999, A&AS, 140, 355
Murgia M., Eckert D., Govoni F., Ferrari C., Pandey-Pommier M., Nevalainen J., Paltani S., 2010a, A&A, 514, A76
Murgia M., Govoni F., Feretti L., Giovannini G., 2010b, A&A, 509, A86
Murgia M. et al., 2011, A&A, 526, A148
Nevalainen J., Eckert D., Kaastra J., Bonamente M., Kettula K., 2009, A&A, 508, 1161
Nulsen P., Jones C., Forman W., Churazov E., McNamara B., David L., Murray S., 2009, in Heinz S., Wilcots E., eds, AIP Conf. Ser. Vol. 1201, The Monster's Fiery Breath. Am. Inst. Phys., New York, p. 198
Nusser A., Silk J., Babul A., 2006, MNRAS, 373, 739
O'Dea K. P. et al., 2010, ApJ, 719, 1619
O'Hara T. B., Mohr J. J., Guerrero M. A., 2004, ApJ, 604, 604
Ogrean G. A., Hatch N. A., Simionescu A., Böhringer H., Brüggen M., Fabian A. C., Werner N., 2010, MNRAS, 406, 354
Otani C., Brinkmann W., Boehringer H., Reid A., Siebert J., 1998, A&A, 339, 693
Owen F. N., Ledlow M. J., 1997, ApJS, 108, 41
Owen F. N., O'Dea C. P., Inoue M., Eilek J. A., 1985, ApJ, 294, L85
Owen F. N., Eilek J. A., Kassim N. E., 2000, ApJ, 543, 611
Owers M. S., Couch W. J., Nulsen P. E. J., 2009a, ApJ, 693, 901
Owers M. S., Nulsen P. E. J., Couch W. J., Markevitch M., 2009b, ApJ, 704, 1349
Owers M. S., Nulsen P. E. J., Couch W. J., 2011, ApJ, 741, 122
Paolillo M., Fabbiano G., Peres G., Kim D.-W., 2003, ApJ, 586, 850
Parma P., de Ruiter H. R., Fanti C., Fanti R., 1986, A&AS, 64, 135
Parrish I. J., Quataert E., Sharma P., 2010, ApJ, 712, L194
Paturel G., Petit C., Prugniel P., Theureau G., Rousseau J., Brouty M., Dubois P., Cambrésy L., 2003, A&A, 412, 45
Paul S., Iapichino L., Miniati F., Bagchi J., Mannheim K., 2011, ApJ, 726, 17
Peletier R. F., Davies R. L., Illingworth G. D., Davis L. E., Cawson M., 1990, AJ, 100, 1091
Peterson J. R. et al., 2001, A&A, 365, L104
Pfrommer C., Chang P., Broderick A. E., 2012, ApJ, 752, 24
Pizzo R. F., de Bruyn A. G., 2009, A&A, 507, 639
Poole G. B., Babul A., McCarthy I. G., Sanderson A. J. R., Fardal M. A., 2008, MNRAS, 391, 1163
Pratt G. W., Croston J. H., Arnaud M., Böhringer H., 2009, A&A, 498, 361
Rafferty D. A., McNamara B. R., Nulsen P. E. J., Wise M. W., 2006, ApJ, 652, 216
Rafferty D. A., McNamara B. R., Nulsen P. E. J., 2008, ApJ, 687, 899
Randall S. W., Clarke T. E., Nulsen P. E. J., Owers M. S., Sarazin C. L., Forman W. R., Murray S. S., 2010, ApJ, 722, 825
Reiprich T. H., Böhringer H., 2002, ApJ, 567, 716
Reiprich T. H., Sarazin C. L., Kempner J. C., Tittley E., 2004, ApJ, 608, 179
Reynolds C. S., Casper E. A., Heinz S., 2008, ApJ, 679, 1181
Roediger E., Brüggen M., Simionescu A., Böhringer H., Churazov E., Forman W. R., 2011, MNRAS, 413, 2057
Roediger E., Lovisari L., Dupke R., Ghizzardi S., Brüggen M., Kraft R. P., Machacek M. E., 2012, MNRAS, 420, 3632
Rossetti M., Molendi S., 2010, A&A, 510, A83
Rossetti M., Eckert D., Cavalleri B. M., Molendi S., Gastaldello F., Ghizzardi S., 2011, A&A, 532, A123
Rottgering H. J. A., Wieringa M. H., Hunstead R. W., Ekers R. D., 1997, MNRAS, 290, 577
Ruszkowski M., Oh S. P., 2010, ApJ, 713, 1332
Sakelliou I., Ponman T. J., 2004, MNRAS, 351, 1439
Sakelliou I., Ponman T. J., 2006, MNRAS, 367, 1409
Sanders J. S., Fabian A. C., Taylor G. B., 2005, MNRAS, 356, 1022
Sanders J. S., Fabian A. C., Taylor G. B., 2009a, MNRAS, 393, 71
Sanders J. S., Fabian A. C., Taylor G. B., 2009b, MNRAS, 396, 1449
Sanderson A. J. R., Ponman T. J., O'Sullivan E., 2006, MNRAS, 372, 1496
Sanderson A. J. R., O'Sullivan E., Ponman T. J., 2009, MNRAS, 395, 764
Sarazin C. L., Burns J. O., Roettiger K., McNamara B. R., 1995a, ApJ, 447, 559
Sarazin C. L., Baum S. A., O'Dea C. P., 1995b, ApJ, 451, 125
Sauvageot J. L., Belsole E., Pratt G. W., 2005, A&A, 444, 673
Sharma P., McCourt M., Quataert E., Parrish I. J., 2012, MNRAS, 420, 3174
Shurkin K., Dunn R. J. H., Gentile G., Taylor G. B., Allen S. W., 2008, MNRAS, 383, 923
Slee O. B., Roy A. L., 1998, MNRAS, 297, L86
Slee O. B., Roy A. L., Murgia M., Andernach H., Ehle M., 2001, AJ, 122, 1172

Smith R. K., Brickhouse N. S., Liedahl D. A., Raymond J. C., 2001, ApJ, 556, L91
Sun M., 2009, ApJ, 704, 1586
Sun M., 2012, New J. Phys., 14, 045004
Sun M., Murray S. S., Markevitch M., Vikhlinin A., 2002, ApJ, 565, 867
Sun M., Jones C., Forman W., Vikhlinin A., Donahue M., Voit M., 2007, ApJ, 657, 197
Takizawa M., Sarazin C. L., Blanton E. L., Taylor G. B., 2003, ApJ, 595, 142
Tanaka N., Furuzawa A., Miyoshi S. J., Tamura T., Takata T., 2010, PASJ, 62, 743
Taylor G. B., Perley R. A., Inoue M., Kato T., Tabara H., Aizu K., 1990, ApJ, 360, 41
Taylor G. B., Barton E. J., Ge J., 1994, AJ, 107, 1942
Tittley E. R., Henriksen M., 2001, ApJ, 563, 673
Tittley E. R., Henriksen M., 2005, ApJ, 618, 227
Vacca V., Govoni F., Murgia M., Giovannini G., Feretti L., Tugnoli M., Verheijen M. A., Taylor G. B., 2011, A&A, 535, A82
van Weeren R. J., Intema H. T., Oonk J. B. R., Röttgering H. J. A., Clarke T. E., 2009, A&A, 508, 1269
van Weeren R. J., Brüggen M., Röttgering H. J. A., Hoeft M., 2011, MNRAS, 418, 230
Venturi T., Bardelli S., Morganti R., Hunstead R. W., 2000, MNRAS, 314, 594
Venturi T., Bardelli S., Zambelli G., Morganti R., Hunstead R. W., 2001, MNRAS, 324, 1131
Venturi T., Bardelli S., Zagaria M., Prandoni I., Morganti R., 2002, A&A, 385, 39
Venturi T., Bardelli S., Dallacasa D., Brunetti G., Giacintucci S., Hunstead R. W., Morganti R., 2003, A&A, 402, 913
Venturi T., Dallacasa D., Stefanachi F., 2004, A&A, 422, 515
Vikhlinin A., Forman W., Jones C., 1997, ApJ, 474, L7
Vikhlinin A., Markevitch M., Murray S. S., 2001a, ApJ, 551, 160
Vikhlinin A., Markevitch M., Forman W., Jones C., 2001b, ApJ, 555, L87
Voit G. M., Cavagnolo K. W., Donahue M., Rafferty D. A., McNamara B. R., Nulsen P. E. J., 2008, ApJ, 681, L5
Wang Y., Xu H., Gu L., Gu J., Qin Z., Wang J., Zhang Z., Wu X., 2010, MNRAS, 403, 1909
Werner N., de Plaa J., Kaastra J. S., Vink J., Bleeker J. A. M., Tamura T., Peterson J. R., Verbunt F., 2006, A&A, 449, 475
Wise M. W., McNamara B. R., Nulsen P. E. J., Houck J. C., David L. P., 2007, ApJ, 659, 1153
ZuHone J. A., Markevitch M., Johnson R. E., 2010, ApJ, 717, 908
ZuHone J., Markevitch M., Brunetti G., 2011a, Mem. Soc. Astron. Ital., 82, 632
ZuHone J. A., Markevitch M., Lee D., 2011b, ApJ, 743, 16

This paper has been typeset from a TEX/LATEX file prepared by the author.